Supplementary Information

Three-Dimensional Heterogeneity in Liquid Electrolyte Structure Promotes Na Ion Transport and Storage Performance For Na-ion Batteries

Mengying Ma,[+ a] *Binbin Chen*,[+ acd] *Huilin Pan** [ab]

*Corresponding authors

[a] Department of Chemistry, Zhejiang University, Hangzhou, 310012, China

E-mail: panhuilin@zju.edu.cn

[b] State Key Laboratory of Clean Energy Utilization, Zhejiang University, Hangzhou, 310012, China

[c] Institute of Bioengineering, College of Chemical and Biological Engineering, Zhejiang University, Hangzhou, 310027, China

[d] ZJU-Hangzhou Global Scientific and Technological Innovation Centre, Hangzhou, 311200, China

[+]These authors contributed equally to this work.

Experimental section

Electrolyte and electrode preparation

The NaFSI (Solvionic, 99.7%) was dried at 80 °C for 12 h in an Ar-filled glovebox before use. TEP (Sigma-Aldrich, 99.8%), $PhCF_3$ (Macklin, 99%) and 1,4-$Ph(CF_3)_2$ (Macklin, 99%) were dehydrated with 4 Å molecular sieves for two days before used. The electrolytes were prepared as below. Firstly, NaFSI was dissolved in TEP to form the HCE, with a NaFSI:TEP molar ratio of 1:1.5. Then, the DHCEs were prepared by adding $PhCF_3$ or 1,4-$Ph(CF_3)_2$ diluents into the HCE with a molar ratio of 1:1.5:2 (NaFSI : TEP : diluent). All the electrolytes were prepared and stored in a glovebox under high-purity Ar gas at room temperature. To prepare electrodes, the HC (or CNFM, $Na_3V_2(PO_4)_3$ (NVP))/super P/polyvinylidene fluoride (PVDF) with a weight ratio of 90:5:5 was blended in N-Methyl-2-pyrrolidone to form slurries. Then, the slurry was cast on Cu foil for the HC anode and Al foil for the CNFM cathode. The electrode was punched into the circular electrode with a diameter of 12 mm and dried at 120 °C under vacuum for 12 h. The mass loading for HC is around 1.3 mg cm^{-2} for half cells and 6.7 mg cm^{-2} for full cells, the mass loading for NVP is around 3.5 mg cm^{-2}, and the mass loading for CNFM is around 14.6 mg cm^{-1}. The N/P ratio employed for the CNFM||HC full cell is 1.09.

Cell fabrication and electrochemical measurements

CR2032 coin cells were used for the CNFM||Na, HC||Na, and CNFM||HC cells, with the glass fibre (Whatman, F-type) as separator and the electrolyte was controlled as 150 μL per cell. All coin cells were assembled with designed electrodes and electrolytes in the glove box. Galvanostatic charge-discharge measurements for cells were performed on the Neware battery test system (MHW-200 shenzhen, china). The CNFM||Na half cells were cycled between 1.8 V and 4.0 V while the CNFM||HC full cells were cycled between 1.0 V and 4.0 V. The cycling performance of HC||Na cells was demonstrated with a fixed discharge capacity of 300 mAh g^{-1} at 0.2 C (25 ºC) or

0.33 C (60 °C), and the charge-discharge voltage profiles were recorded to evaluate the degradation of the Na^+ storage in HC electrodes at different temperatures. CV measurements were conducted for HC and CNFM electrodes using an electrochemical workstation (VSP300, BioLogic, France) at sweep rates of 0.2 mV s^{-1} in the voltage range of 0-3 V (HC) and 1.5-4 V (CNFM) versus Na/Na^+. Operando-EIS for CNFM||HC full cells were performed using VSP300 in a frequency range of 7×10^6~5×10^{-3} Hz at 25 °C.

Characterizations

The ionic conductivity of electrolytes was measured using a Mettler Toledo conductivity meter (S230, Cond probe InLab 751) in the temperature range of 0 to 50 °C. The Na^+ transference number was evaluated utilizing Na || Na symmetric cell combined by EIS before and after the chronoamperometry (CA) test and calculated by the following equation (1)[1]:

$$t_{Na^+} = {I_{ss}(\Delta V - I_0 R_0)}/{I_0(\Delta V - I_{ss} R_{ss})} \quad (1)$$

Where I_0 and I_{ss} are the initial current and steady-state current, respectively, ΔV is the applied voltage polarization (10 mV), R_0 and R_{ss} are the electrode resistances before and after the polarization, respectively. The DSC tests were used to determine the phase evolution of the electrolytes in a temperature range of -70~20 °C with temperature change rate of 10 °C min^{-1}. NMR (Avance-400) and Raman (Renishaw inVia) measurements were employed to investigate the local solvation structure of the as-prepared electrolytes. The microstructures of the HC and CNFM electrodes were obtained using HRTEM (JEM 2100F). XPS measurements were performed using Thermo Scientific K-Alpha. The C 1s peak (284.8 eV) was employed as the reference to calibrate the position of other peaks. The postmortem analysis of electrodes for the XPS and HRTEM were obtained from CNFM||HC full cells after the first cycle.

Molecular dynamics simulation

The classical MD simulations were performed by GROMACS 5.0 software.[2] The amber force field parameters needed for this study were obtained from Gaussian and acpype.[3] Three systems consisting of 100 NaFSI/150 TEP, 100 NaFSI/150 TEP/200 $PhCF_3$, and 100 NaFSI/150 TEP/200 1,4-$Ph(CF_3)_2$ were simulated in different boxes using periodic boundary conditions. The force field parameters of Na^+, TEP, and FSI^- were referred to the previous publications.[4] First, the simulation box was initially set as a cube with a length of 10 nm. Then, the systems were preliminarily equilibrated by 0.1 ns energy minimization, as well as 1 ns canonical ensemble (NVT) and 2 ns isothermal-isobaric ensemble (NPT) ensemble simulations. Finally, after further 10 ns MD simulations, the simulation boxes shrank to a suitable size and the systems reached a stable state. During all simulations, the constant temperature (298 K) and the constant pressure (1.0 bar) coupling were maintained by Nose-Hoover thermostat[5] and Parrinello-Rahman pressure,[6] respectively. Linear constraint solver algorithm was used to constrain bond lengths in our simulations.[7] The cut-off of non-bonded van der Waals interaction and long-range electrostatic interaction were both set at 1.2 nm for all systems. All RDF curves were calculated by GROMACS5.0, and the RDF curves were visualized with visual molecular dynamics (VMD)[8] in this study. The coordination number mentioned in this manuscript refers to the coordination number of Na^+ in the electrolyte, which is the total number of neighboring atoms of the centered Na^+ ion in the electrolyte. The coordination ratios for different species in different coordination shells are calculated as follows:

In HCE and two DHCEs, FSI^- anion exhibits multi-coordination sites from oxygen, nitrogen and sulfur atoms of FSI^- anion. Therefore, the FSI^- anions could contribute a large percentage of coordination ratio around Na^+.

The coordinate numbers (N) of Na^+ in different electrolytes are obtained from the formula (1):

$$N=4\pi\rho\int_0^r r^2 g(r)dr,\quad \rho=\frac{n}{V} \qquad (1)$$

in which r is the radius, g(r) is the radial distribution function, n is the specific numbers of the components in the system, V is the system volume.

In addition, the ratios of different components in the coordination shell x_i are calculated according to the formula (2):

$$x_i = \frac{N_i}{\sum N_i} \qquad (2)$$

The first to the third coordination shells are considered for r=0.1-0.3 nm, r=0.3-0.5, and r=0.5-1.0 nm, respectively.

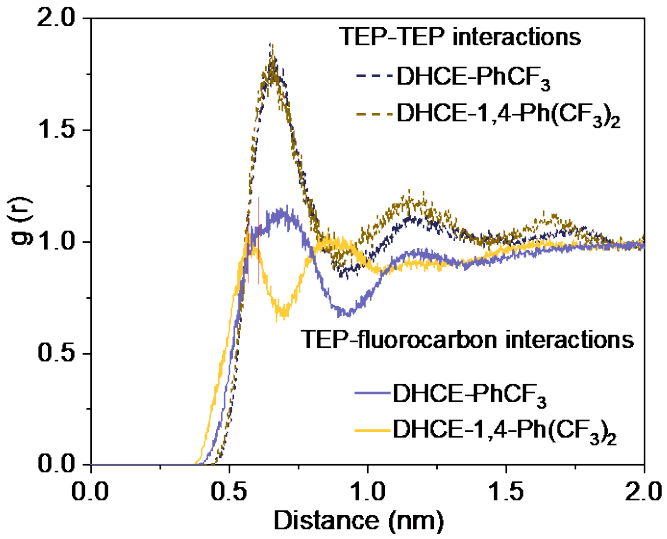

Figure S1. RDF curves for TEP-TEP interactions and TEP-fluorocarbon interactions in different DHCEs extracted from MD simulations (All the RDF curves in this figure take the centroid of TEP molecule as the reference center).

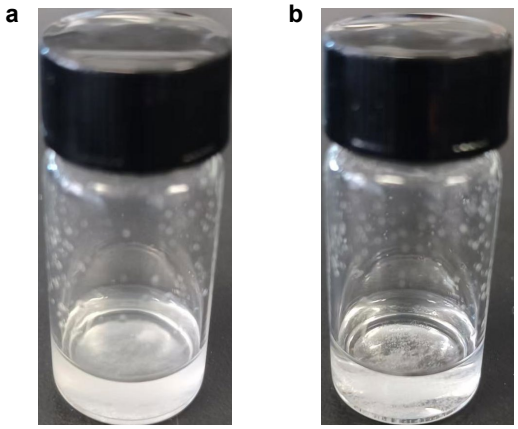

Figure S2. Images of 0.05 M NaFSI in (a) $PhCF_3$ and (b) 1,4-$Ph(CF_3)_2$.

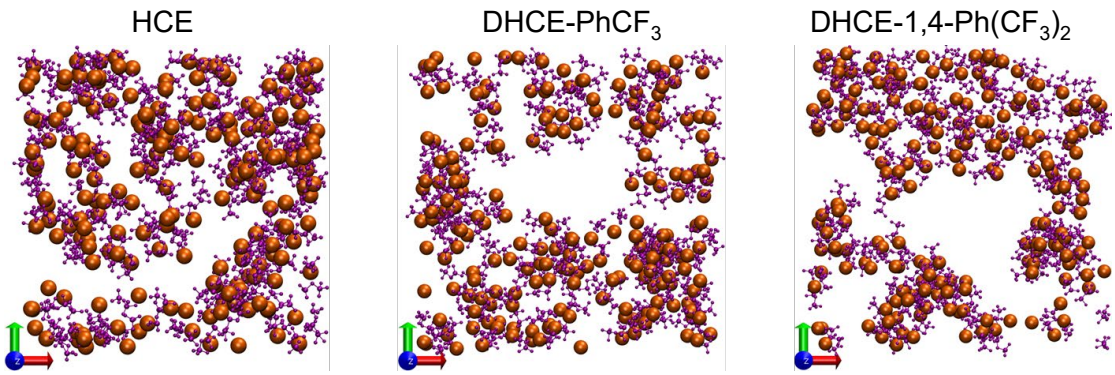

Figure S3. Long-range bonding structure of Na^+-FSI^- in different electrolytes. Almost all FSI^- participate in the solvation with Na^+. FSI^- and Na^+ are shown in purple and orange, respectively.

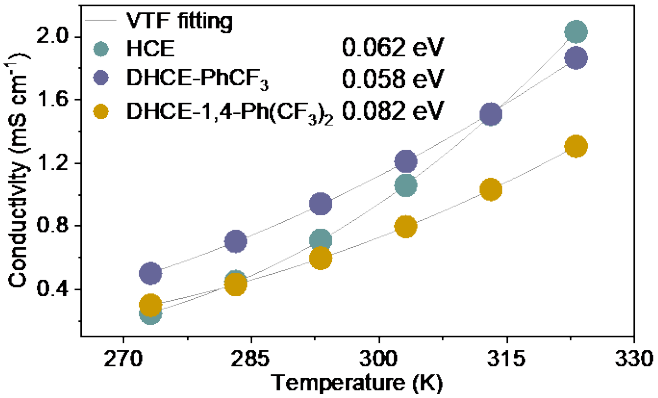

Figure S4. Fitting of activation energies for different electrolytes using Empirical Vogel-Tamman-Fulcher (VTF) equation.

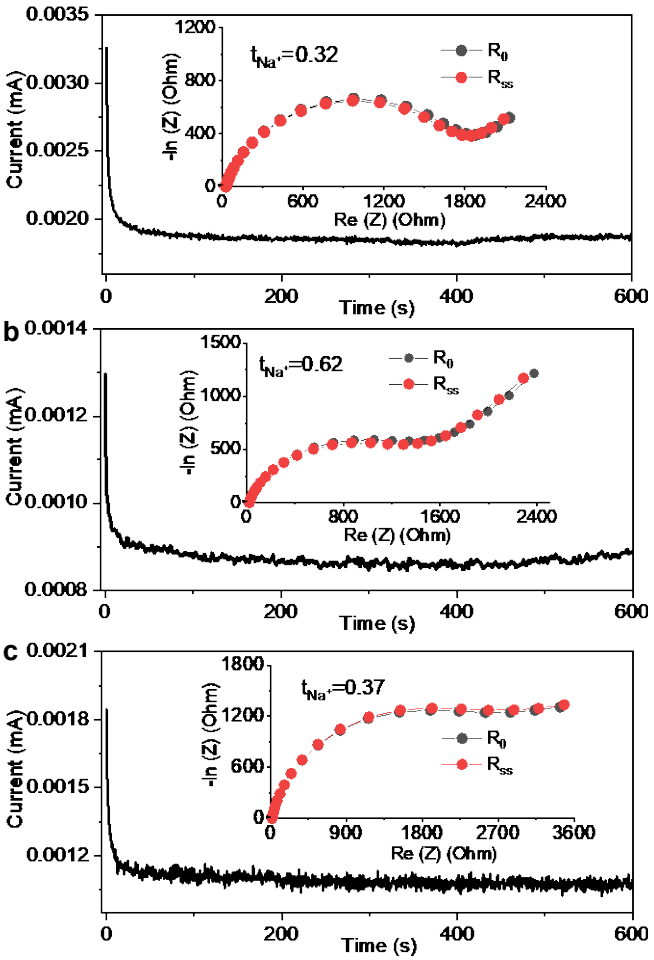

Figure S5. Characterization of Na^+ transference number in (a) HCE, (b) DHCE-$PhCF_3$ and (c) DHCE-1,4-$Ph(CF_3)_2$. Current variations with the polarization of Na||Na symmetric cells with an applied potential of 10 mV and EIS tests before and after polarization in different electrolytes.

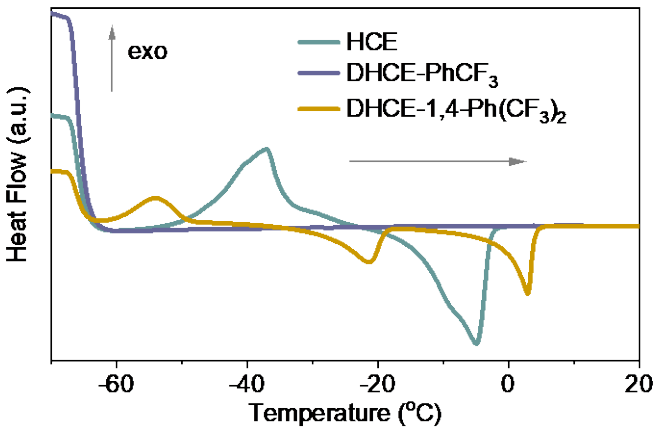

Figure S6. DSC thermograms at heating scan of HCE, DHCE-$PhCF_3$ and DHCE-1,4-$Ph(CF_3)_2$ in the temperature range of -70 to 20 °C.

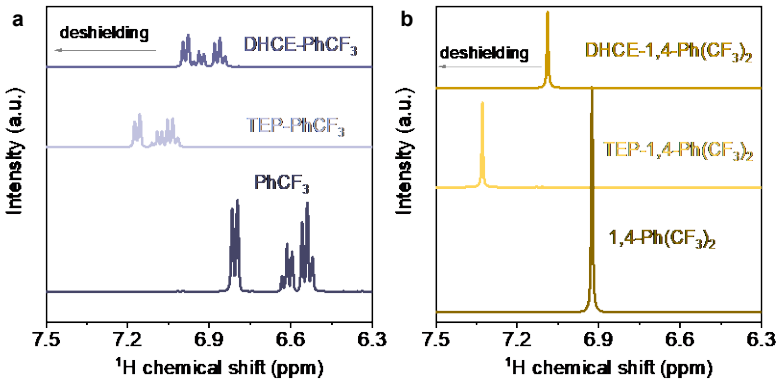

Figure S7. ^{1}H-NMR chemical shifts of benzene ring in (a) pure $PhCF_3$, TEP-$PhCF_3$ mixed solvent and DHCE-$PhCF_3$ and (b) 1,4-$Ph(CF_3)_2$, TEP-1,4-$Ph(CF_3)_2$ mixed solvent and DHCE-1,4-$Ph(CF_3)_2$.

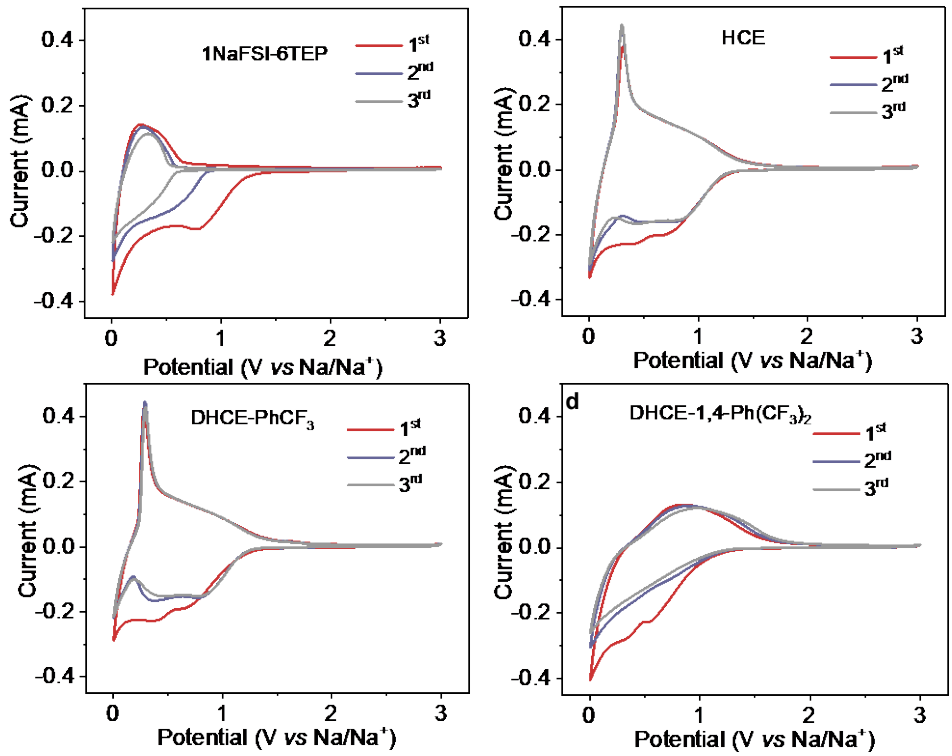

Figure S8. The CV curves of HC anodes at a scan rate of 0.2 mV s^{-1} in (a) dilute 1NaFSI-6TEP, (b) HCE, (c) DHCE-$PhCF_3$, and (d) DHCE-1,4-$Ph(CF_3)_2$.

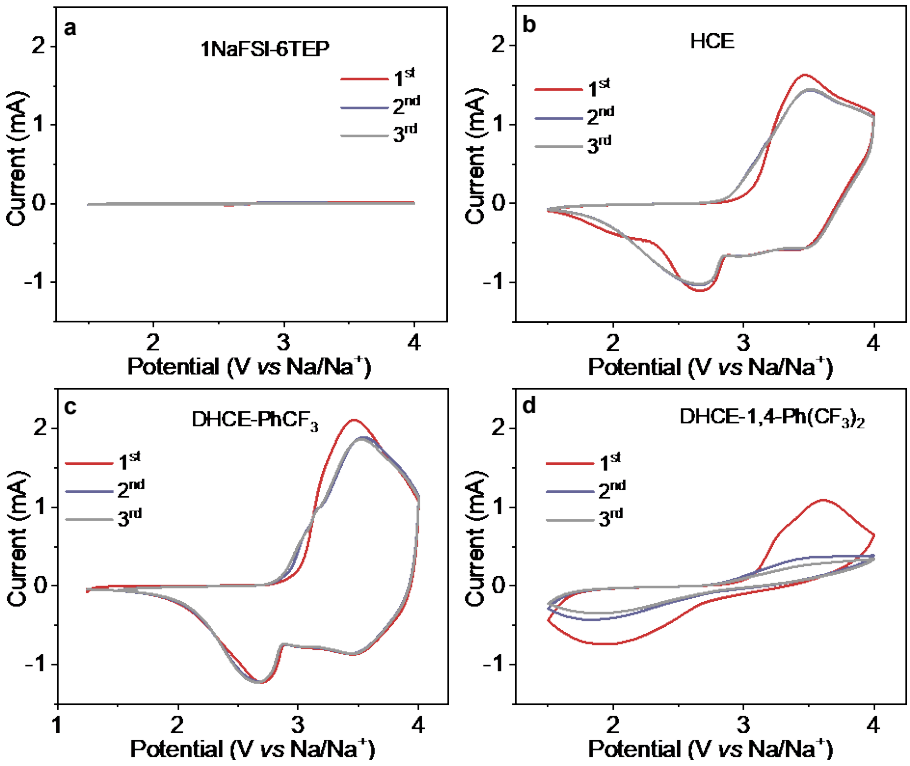

Figure S9. The initial CV curves of CNFM cathodes at a scan rate of 0.2 mVs^{-1} in (a) dilute 1NaFSI-6TEP, (b) HCE, (c) $DHCE\text{-}PhCF_3$, and (d) $DHCE\text{-}1,4\text{-}Ph(CF_3)_2$.

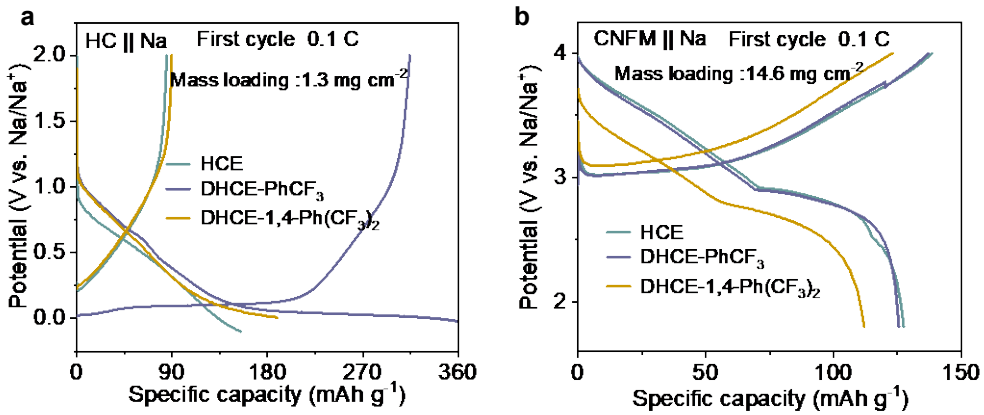

Figure S10. Typical charge-discharge curves of half cells at 0.1 C in different electrolytes of the (a) HC||Na and (b) CNFM||Na.

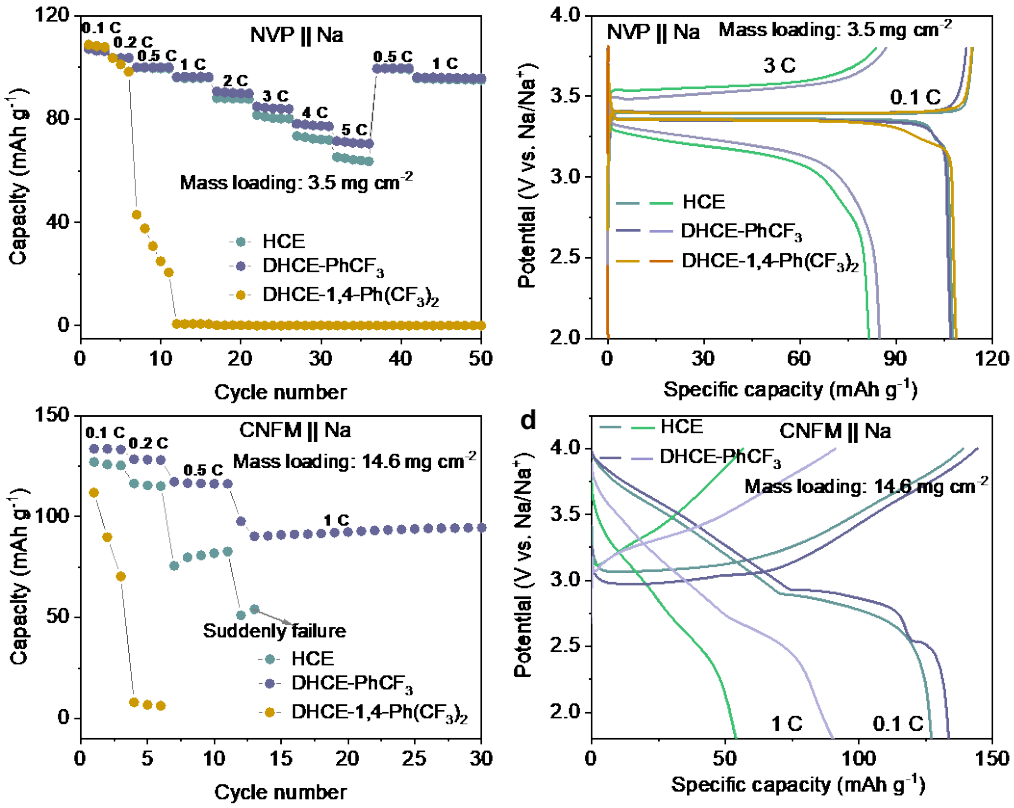

Figure S11. The rate performance of NVP||Na half cells (a,b) and CNFM||Na half cells (c,d) in different electrolytes.

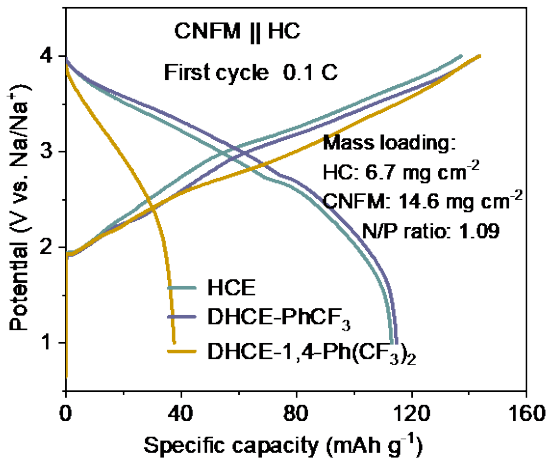

Figure S12. Typical charge-discharge curves CNFM||HC full cells at 0.1 C in different electrolytes.

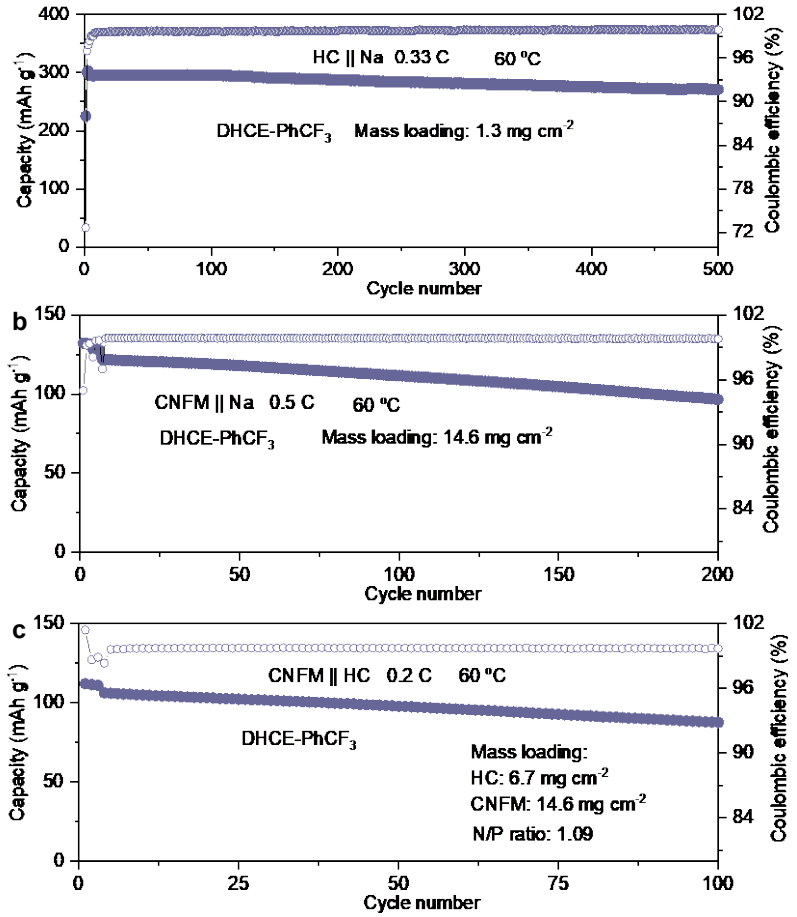

Figure S13. High-temperature cycling performance of (a) HC || Na half cell (b) CNFM || Na half cell and (c) CNFM || HC full cell in DHCE-$PhCF_3$ at 60 °C.

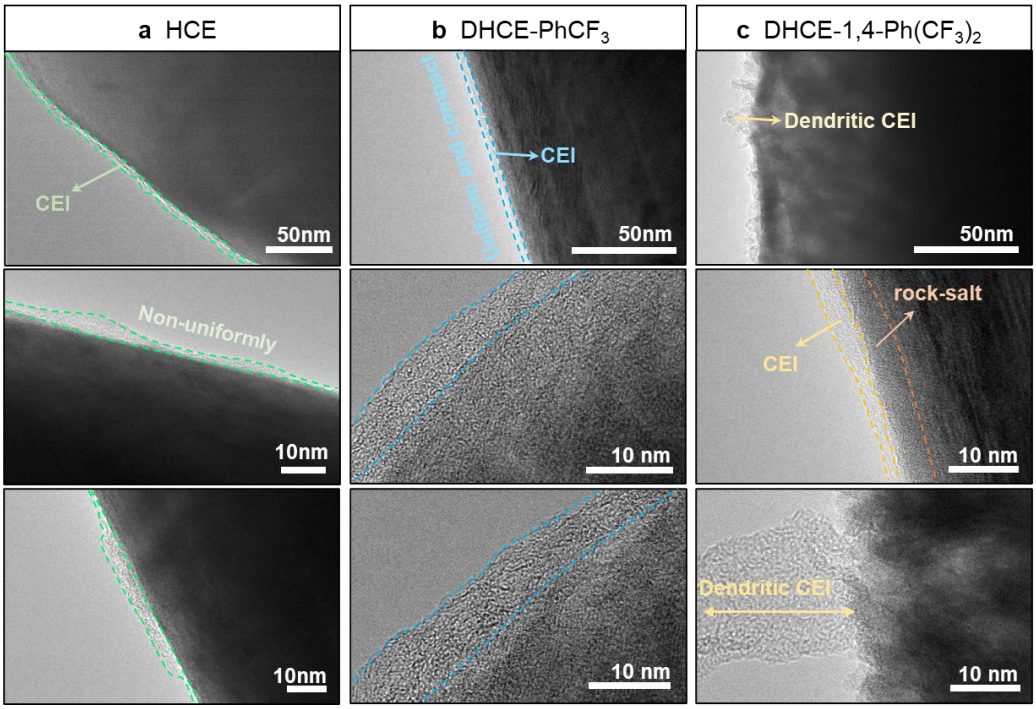

Figure S14. HRTEM images of the CNFM cathodes cycled in (a) HCE, (b) DHCE-PhCF$_3$ and (c) DHCE-1,4-Ph(CF$_3$)$_2$.

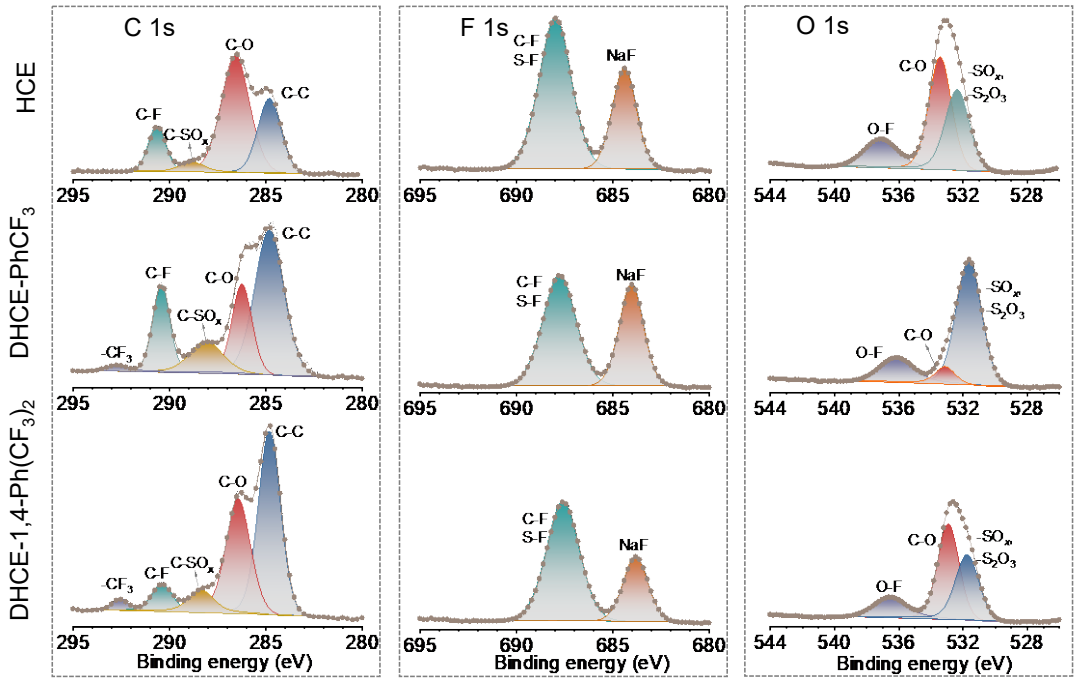

Figure S15. XPS spectra of selected elements of the SEIs on HC anodes after first cycle in the studied electrolytes: (a) C 1s, (b) F 1s, (c) O 1s.

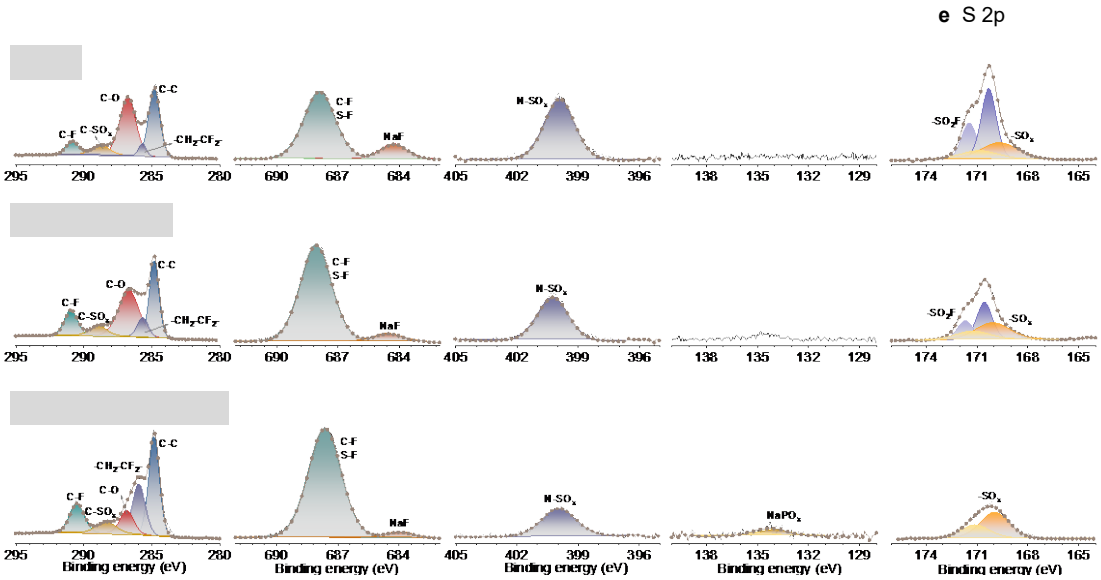

Figure S16. XPS spectra of selected elements of the CEIs on CNFM cathodes after first cycle in the studied electrolytes: (a) C 1s, (b) F 1s, (c) N 1s, (d) P 2p, (e) S 2p.

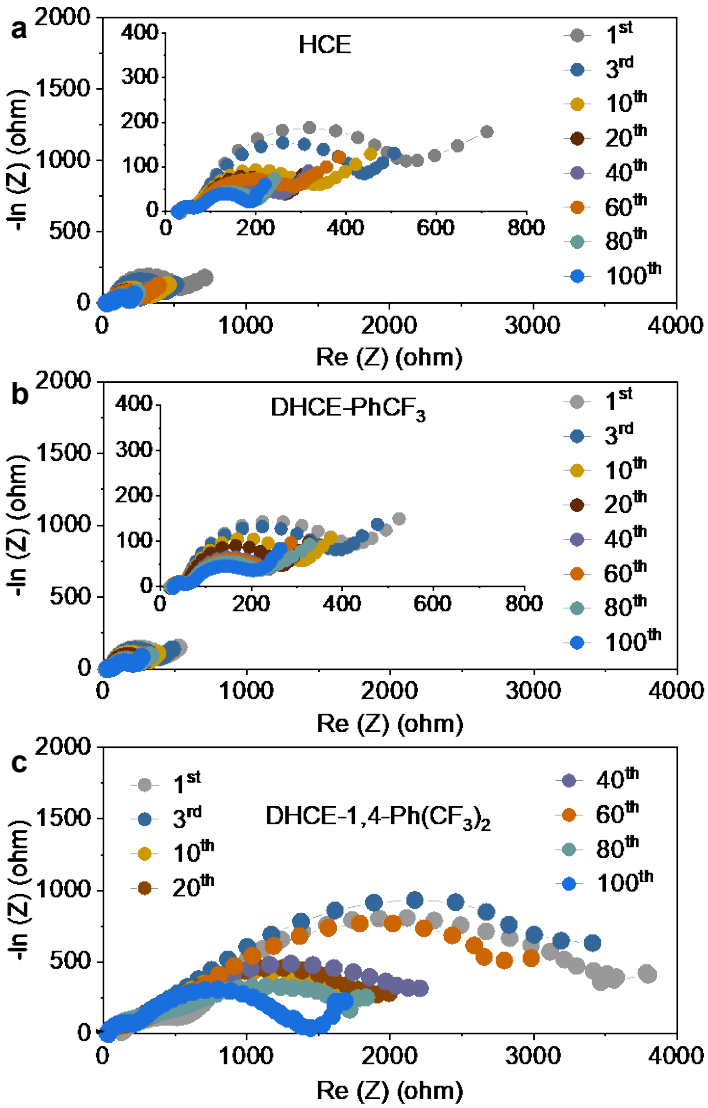

Figure S17. Operando-EIS of the CNFM||HC full cells during cycling in (a) HCE, (b) DHCE-$PhCF_3$, and (c) DHCE-1,4-$Ph(CF_3)_2$.

Table S1. The coordination numbers of different electrolytes at different solvation sheaths extracted from MD simulations.

Electrolyte	Coordination number		
	1^{st} (0-0.3 nm)	2^{nd} (0-0.3 nm)	3^{rd} (0-0.3 nm)
HCE	6.03	16.43	82.86
DHCE-$PhCF_3$	5.86	15.78	79.06
DHCE-1,4-$Ph(CF_3)_2$	5.93	16.37	89.60

Reference

1. P. G. Bruce and C. A. Vincent, *J. electroanal. Chem.*, 1987, **225**, 1-17.
2. M. J. Abraham, T. Murtola, R. Schulz, S. Páll, J. C. Smith, B. Hess and E. Lindahl, *SoftwareX*, 2015, **1-2**, 19-25.
3. A. W. Sousa da Silva and W. F. Vranken, *BMC Res. Notes*, 2012, **5**, 367.
4. M. Ma, B. Chen, X. Yang, Y. Liu, S. Dai, X. Qi, Y.-S. Hu and H. Pan, Solvent Reorganization and Additives Synergistically Enable High-Performance Na-Ion Batteries, *ACS Energy Lett.*, 2022, **8**, 477-485.
5. H. J. C. Berendsen, J. P. M. Postma, W. F. Vangunsteren, A. Dinola and J. R. Haak, Molecular dynamics with coupling to an external bath, *J. Chemical Physics*, 1984, **81**, 3684-3690.
6. R. Martonák, A. Laio and M. Parrinello, Predicting crystal structures: the Parrinello-Rahman method revisited, *Phys. Rev. Lett.*, 2003, **90**, 075503.
7. B. Hess, H. Bekker, H. J. C. Berendsen and J. Fraaije, LINCS: A linear constraint solver for molecular simulations, *J. Comput. Chem.*, 1997, **18**, 1463-1472.
8. W. Humphrey, A. Dalke and K. Schulten, VMD: Visual molecular dynamics, *J. Mol. Graph. & Model.*, 1996, **14**, 33-38.